Role of Brownian Motion Hydrodynamics on Nanofluid Thermal Conductivity

W Evans, J Fish and P Keblinski

⎯ NOTICE ⎯

Role of Brownian Motion Hydrodynamics on Nanofluid Thermal Conductivity

William Evans[1,2], Jacob Fish[2] and Pawel Keblinski[3]

[1] Lockheed Martin Corporation, Niskayuna, NY

[2] Mechanical Engineering Department, Rensselaer Polytechnic Institute, Troy NY

[3] Materials Science and Engineering Department, Rensselaer Polytechnic Institute, Troy NY

Abstract:

We use a simple kinetic theory based analysis of heat flow in fluid suspensions of solid nanoparticles (nanofluids) to demonstrate that the hydrodynamics effects associated with Brownian motion have a minor effect on the thermal conductivity of the nanofluid. Our conjecture is supported by the results of molecular dynamics simulations of heat flow in a model nanofluid with well-dispersed particles. Our findings are consistent with the predictions of the effective medium theory as well as with recent experimental results on well dispersed metal nanoparticle suspensions.

In the last decade, significant research effort was committed to thermal transport properties of colloidal suspensions of nanosized solid particles (nanofluids). [1] Experiments demonstrated that thermal conductivity increases with increasing volume fraction of nanoparticles are dramatically more significant than one would predict from the effective medium theory of a composite material comprised of well-dispersed particles. [2, 3, 4]

A number of possible factors responsible for this behavior were proposed [5, 6, 7, 8] with a consensus yet to emerge. [9] In particular, several authors [6, 7, 8] argued that large thermal conductivity increases are due to hydrodynamic effects of Brownian motion of nanoparticles. The argument first pointed to the well-known continuum hydrodynamic solution of the problem of a sphere moving at constant velocity in fluid. This solution is characterized by a long range velocity field, V(**r**), that decays approximately as the inverse of the distance from the particle center, V(**r**) ~ 1/r. The ability of large volumes of fluid dragged by nanoparticles to carry substantial amounts of heat was credited to be responsible for large thermal conductivity increases of nanofluids.

In this paper we will discuss a kinetic theory based argument suggesting that the Brownian motion contribution to the thermal conductivity of nanofluid is very small and can not be responsible for extraordinary thermal transport properties of nanofluids. We will support our argument with the results of molecular dynamics simulations of a model nanofluid. These results are in good agreement with the predictions of the effective medium theory on composites with well-dispersed particles, as well as with the result of recent thermal transport measurements on nanofluids with well-dispersed metal nanoparticles. [10]

In our considerations we will limit ourselves to stationary fluids, i.e., fluids without macroscopic fluid flow. To provide an estimate for the contribution of the Brownian motion induced nanoscale fluid flow to thermal conductivity we assume that all volume of the fluid diffuses together with the nanoparticles and that the velocity of the fluid is the same as the velocity of the particles. Under such assumptions, which clearly overestimate the actual magnitude of the fluid velocity field, a well-known kinetic theory formula gives Brownian motion induced contribution to the thermal conductivity, κ_B, as:

$$\kappa_B = D_B c_p, \tag{1}$$

where, c_p is the heat capacity of the fluid per unit volume at constant pressure, and D_B is the diffusivity of the nanoparticles. We note that at low particle volume fraction the heat carried by the particles themselves is much lower than the heat carried by the fluid moving together with particles due to the much higher volume of the fluid. Therefore we will neglect the direct contribution of particle Brownian motion to thermal transport.

Thermal conductivity of the base fluid, κ_F, can be also written in the form of Eq. 1 as:

$$\kappa_F = D_T c_p, \tag{2}$$

where, D_T is the thermal diffusivity of the fluid defined as: $D_T = \kappa_F / c_p$.

The ratio of κ_B to κ_F can be evaluated by combining Eqs. 1 and 2,

$$\kappa_B / \kappa_F = D_B / D_T, \tag{3}$$

i.e., the ratio of the thermal conductivity of the Brownian motion contribution to the thermal conductivity of the base fluid is given by the ratio of the nanoparticle diffusivity to the fluid thermal diffusivity.

As a numerical example we consider a water suspension of radius R= 5 10^{-9} m

nanoparticles at room temperature at which water thermal diffusivity is $D_T = 1.4 \ 10^{-7}$ m^2/s and viscosity $\eta = 10^{-3}$ kg/m-s. From the Stokes-Einstein formula, $D_B = k_B T/6\pi\eta R$, which, with the Boltzmann's constant $k_B = 1.4 \ 10^{-23}$ J/K, gives the nanoparticle diffusivity, $D_B = 4.5 \ 10^{-11} \ m^2/s$. These numbers lead to the ratio of thermal conductivities $\kappa_B/\kappa_F = D_B/D_T = 3.2 \ 10^{-4}$.

This very small ratio of κ_B/κ_F (<1%) shows that the Brownian motion induced nanoscale fluid flow has a negligible effect on thermal transport and certainly cannot explain 10% or larger increases of κ_F observed in experiments on nanofluids with very low volume fraction of particles. [2, 3, 4] From the above considerations, it is also clear why the Brownian motion is not important for thermal transport. Simply, the heat motion via a conduction mechanism, quantified by the thermal diffusivity, is much faster than the nanoparticle motion, quantified by the particle diffusivity.

To provide further support for our argument we performed molecular dynamics simulations of heat flow in a model nanofluid comprised of crystalline nanoparticles embedded in a fluid. The interactions between fluid atoms are described by the standard Lennard-Jones (LJ) potential, with pair interaction energy $U_{LJ}(r) = 4\varepsilon[(\sigma/r)^{12} - (\sigma/r)^6]$ where ε and σ are the units of energy and length, respectively. For computational efficiency we selected a cutoff distance $R_C = 2^{1/6}\sigma$, which is at the minimum of the LJ potential. Consequently, all fluid interactions are purely repulsive.

The solid particles are formed by carving spheres out of an fcc lattice of atoms. These atoms, in addition to the repulsive LJ interaction, are connected with the nearest neighbors by attractive springs described by a FENE potential [11] $U_{FENE} = -5.625\varepsilon \ln[1 - (r/1.5\sigma)^2]$. The selected number of atoms in each particle is 296,

4

leading to a radius, $R \approx 4\sigma$. To mimic solid particles, the masses of atoms forming nanoparticles are 3 times larger than the mass of the fluid atom, resulting in a particle density about 4.5 times larger than the fluid density.

In a model nanofluid 8 particles are dissolved in 50,000 fluid atoms (see Figure 1) at a pressure corresponding to the density of pure fluid density of 0.81 particles per σ^3. The corresponding periodic cubic simulation box sizes are about 40 σ, i.e., 10 times the particle radius. This choice leads to a nanofluid with a particle volume fraction of about 3.3%.

The cross interactions between fluid and solid particles are also described by the LJ potential but with a cutoff of 1.5 σ leading to attractive forces between fluid and solid particles. The LJ potential is modified such that both energy and force are equal to zero at the cutoff distance [12]. Three solid-fluid interactions strengths were used, $\varepsilon_{SF} = 0.25\varepsilon$, 1.25$\varepsilon$, and 2.25$\varepsilon$, where ε is the LJ energy unit used in the definition of interactions between fluid atoms. These three choices lead to a range of wetting properties, and are referred throughout as no-wetting, weakly-wetting, and wetting particle cases, respectively.

Before thermal transport simulations each structure was equilibrated for 200,000 MD steps at constant volume and temperature, $T=1.0\varepsilon/k_B$. A MD time step of $0.005\,\tau_{MD}$ ($\tau_{MD} = \sqrt{\varepsilon/m\sigma^2}$, where m is the fluid atom mass) and the Verlet integration algorithm are used in all simulations [12].

To determine thermal conductivity we use the so-called direct method where the planar heat source and sink are applied with the overall thermostat turned off. The sink and source planar regions are both 1 σ wide and are located at the center and at the edge

of the periodic simulation box, as shown in Figure 1. Atomic velocities were scaled up (down) in the heat source (sink) regions so that heat was added at a constant rate of dQ/dt $= 200\varepsilon/\tau_{MD}$, to the source and removed at the same rate from the sink. We monitored the temperature profile along the z direction by calculating the total kinetic energy of the atoms (both solid and fluid) in 1 σ.

Upon the application of the heat source and sink, a steady state temperature profile is established after ~ 100,000 MD steps after which we collect the average temperature profile data over another 100,000 MD steps. Examples of such obtained temperature profiles are shown in Fig. 1 (top panel). The profile is piece-wise linear allowing us to obtain thermal conductivity of the nanofluid, κ_{NF}, using the Fourier's law, $j_Q = -\kappa \partial T/\partial z$, where $j_Q = (dQ/dt)/2A$ is the heat flux, with A being the cross-sectional area (the factor of 2 accounts for heat flow in both positive and negative z-directions in periodic systems). We note that we did not observe any persistent clustering during our simulations, and the particles maintained good dispersion in a fluid throughout the simulation run.

Our key thermal transport results are presented in Table I, showing thermal conductivity of three nanofluids in the reduced LJ units, $k_B/\sigma\sqrt{\varepsilon/m\sigma^2}$, where k_B is the Boltzmann constant. For the reference condition, we also simulated pure fluid for which we obtained, $\kappa_F = 6.33$. In all cases we observed only minor increases of thermal conductivity compared to that of the pure fluid. Also, the thermal conductivity of nanofluids with non-wetting and weakly wetting particles is slightly lower that that of the nanofluid with wetting particles. However, even with wetting particles the thermal conductivity increase is rather minor and does not correspond to spectacular increases

observed in experiment [2, 3, 4].

The differences in thermal conductivity of the three model nanofluids originate from the interfacial thermal resistance of the solid-fluid interface [13]. We evaluate this resistance by MD simulations in which a single particle is heated at a constant rate and the heat is removed from a spherical shell away from the particle. The resulting radial temperatures profiles are shown in Figure 2. The profiles in the fluid are essentially the same and follow the well-known solution of the steady state heat flow problem with spherical symmetry, T = B +A/r, where B and A are constants related to the magnitude of generated heat and fluid thermal conductivity. However, at the solid fluid interface there is a discontinuous temperature jump associated with interfacial thermal resistance, which is particularly large for the no-wetting particle case [14]. From the data in Figure 2 we evaluated the so-called equivalent matrix thickness h, (see Table I) over which the temperature drop is the same as at the interface in the planar heat flow geometry.

Knowledge of the interfacial thermal resistance, particle size, and volume fraction allows estimation of the nanofluid conductivity according to the effective medium theory that at low volume fractions of well-dispersed thermally conductive nanoparticles, predicts [12];

$$\frac{\kappa_{NF}}{\kappa_F} = 1 + 3f\frac{\gamma - 1}{\gamma + 2}, \qquad (4)$$

where f is the particle volume fraction, and γ is the ratio of the particle radius to the equivalent matrix thickness h. According to Equation 4 with no interfacial resistance ($\gamma \to \infty$) the ratio κ_{NF}/κ_F has a maximum value of $1+3f$. When the particle radius becomes equal to the equivalent matrix thickness ($\gamma = 1$) there is no thermal conductivity

enhancement at all, while for larger interfacial resistance ($\gamma < 1$) the addition of particles decreases the thermal conductivity of the fluid, as particles act as insulating holes.

The results of our simulations are in good agreement with Equation 4 as shown by the data in Table I. In all cases, due to non-zero interfacial resistance, the nanofluid conductivity is below $1+3f = 1.1$. The conductivity is the highest for the fluid with wetting particles with the smallest interfacial resistance and lower for the other two cases characterized by a higher interfacial thermal resistance.

In summary, we presented a kinetic theory argument and results of molecular dynamics simulations, both leading to a conclusion that thermal conductivity of a nanofluid with well dispersed nanoparticles is well described by the effective medium theory and do not show any significant enhancements due to effects associated with Brownian motion of nanoparticles. Our conclusions are in agreement with results of recent experiments on thermal conductivity of suspension of well-dispersed metal nanoparticles [10].

Table 1: Thermal transport data of the nanofluids with no-wetting (ε_{SF}=0.25) , weakly-wetting (ε_{SF}=1.25), and wetting particle (ε_{SF}=2.25). Interfacial resistance in units if the equivalent fluid thickness, h, nanofluid thermal conductivity, κ_{NF}, in reduced LJ units. Ratios κ_{NF}/κ_F obtained form MD simulations with κ_F=6.33 are compared against the predictions of the effective medium theory (Eq. 4).

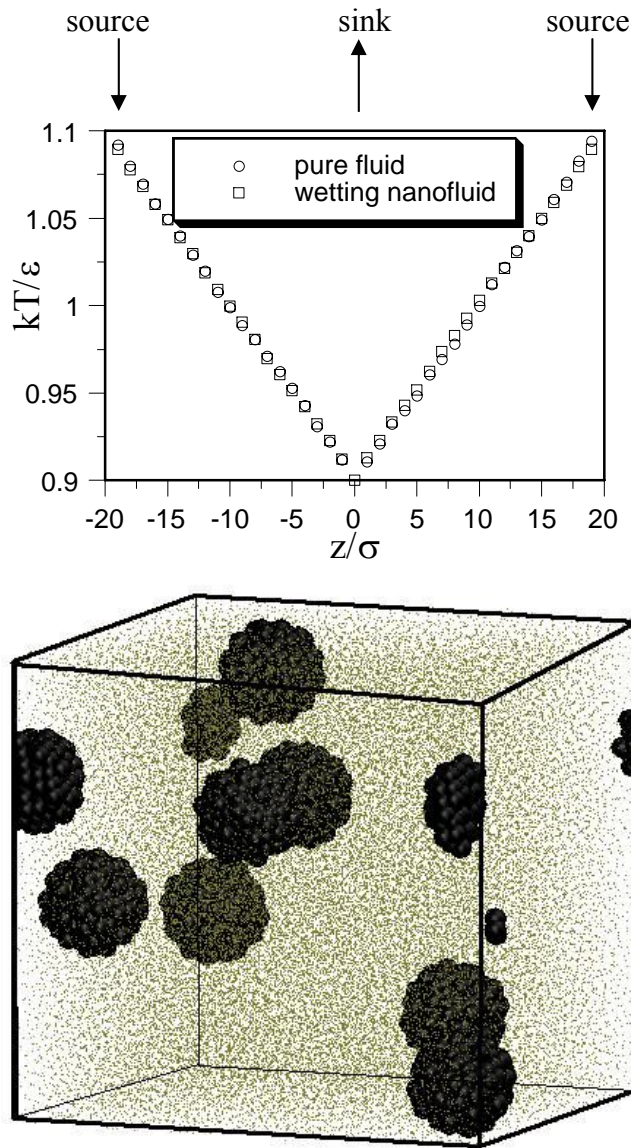| ε_{SF} Interaction Strength	h Equivalent Matrix Thickness	κ_{NF} MD Results	$\dfrac{\kappa_{NF}}{\kappa_F}$ MD Results	$\dfrac{\kappa_{NF}}{\kappa_F}$ Effective Medium Theory
0.25	5.2	6.39	1.0095	0.9917
1.25	3.8	6.39	1.0095	1.0017
2.25	1.8	6.48	1.025	1.0286

Figure 1: Bottom panel: A snapshot of atomic positions of the nanofluid model structure comprising of 8 crystalline nanoparticles embedded in a liquid. Top panel: Temperature profiles obtained from the heat source-sink simulations for pure melt and wetting particle nanofluid. The slope of the temperature profile allows determining thermal conductivity. The arrows indicate positions of the heat source and sink.
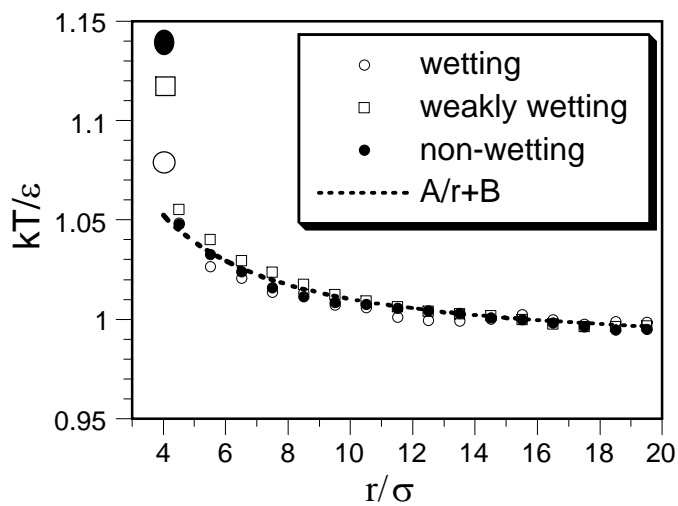
Figure 2: Radial temperature profiles from the simulations in which a single particle is heated by a constant heat source and the heat is removed from a spherical shell at distance 20 σ away from the particle center. Presented data are for non-wetting, weakly wetting and wetting nanoparticles. Larger symbols represent temperatures of the particles. The dotted line is a fit to the $T = A/r + B$ formula.

References:

[1] For a recent review see J. A. Eastman, S. R. Phillpot, S. U.-S. Choi, and P. Keblinski, *Annual Review of Materials Research* **34**, 219 (2004).

[2] J.A. Eastman *et. al., Appl. Phys. Lett.* **78**, 718 (2001).

[3] H. E. Patel, *et al., Appl. Phys. Lett.* **83**, 2931 (2003)

[4] T-K Hong, H-S Yang, C. J. Choi, *J. Applied Physics* **97**, 64311 (2005).

[5] P. Keblinski *et. al, Int J. Heat Mass Trans.* **45**, 855 (2002).

[6] S.P. Jang and S.U.S. Choi, *Appl. Phys. Lett.* **84**, 4316 (2004).

[7] R. Prasher *et. al*., Phys. Rev. Lett. **94**, 025901, (2005).

[8] J. Koo and C. Kleinstreuer, *J. Nanoparticle Research* **6**, 577 (2004)

[9] P. Keblinski, J.A. Eastman, and D.G. Cahill, *Materials Today*, **8,** 36. (2005)

[10] S. A. Putnam, D. G. Cahill, P. V. Braun Z. Ge, and R. G. Shimmin, submitted, available at: http://users.mrl.uiuc.edu/cahill/preprints.html

[11] G. S. Grest, and K. Kremer, J. Chem. Phys. **92**, 5057 (1990) and references therein.

[12]M. P. Allen and D. J. Tildesley, *Computer Simulation of Liquids* (Oxford University Press, Oxford, 1992).

[13] S. A. Putnam, *et al*., *J. Appl. Phys*. **94**, 6785 (2003).

[14] L. Xue, P. Keblinski, S. R. Phillpot, S. U.-S. Choi, and J. A. Eastman, *J. Chem. Phys*. **118**, 337 (2003).